Truth cube: Establishing physical standards for soft tissue simulation

Amy E. Kerdok[a,*], Stephane M. Cotin[b], Mark P. Ottensmeyer[b], Anna M. Galea[a],
Robert D. Howe[a], Steven L. Dawson[b]

[a]*Division of Engineering and Applied Sciences, Harvard University, Cambridge, MA, USA*
[b]*CIMIT Simulation Group, Massachusetts General Hospital, Boston, MA, USA*

Abstract

Accurate real-time models of soft tissue behavior are key elements in medical simulation systems. The need for fast computation in these simulations, however, often requires simplifications that limit deformation accuracy. Validation of these simplified models remains a challenge. Currently, real-time modeling is at best validated against finite element models that have their own intrinsic limitations. This study develops a physical standard to validate real-time soft tissue deformation models. We took CT images of a cube of silicone rubber with a pattern of embedded Teflon spheres that underwent uniaxial compression and spherical indentation tests. The known material properties, geometry and controlled boundary conditions resulted in a complete set of volumetric displacement data. The results were compared to a finite element model analysis of identical situations. This work has served as a proof of concept for a robust physical standard for use in validating soft tissue models. A web site has been created to provide access to our database: http://biorobotics.harvard.edu/truthcube/ (soon to be http://www.truthcube.org).
© 2003 Elsevier B.V. All rights reserved.

Keywords: Physical standard; Real-time models; Model validation; Soft tissue mechanics; Surgical simulation

1. Introduction

Fast, realistic mechanical modeling of soft tissues remains a formidable challenge in the development of new medical applications. Simulations used in medical training, surgical planning, and image-guidance systems require real-time calculation of soft tissue deformation and interaction forces during manipulation of the simulated tissue. For soft tissue simulation to become a practical reality, further investigation of tissue biomechanical parameters, development of more efficient and accurate computer algorithms, and validation of simulated deformations against real in vivo data need to be addressed (Delingette, 1998).

Implementing modeling systems has proved difficult mainly due to the tradeoff between fast computation time and calculated deformation accuracy. Depending on the simulation's desired application, emphasis can be shifted towards the real-time aspect (e.g., surgical procedure training) or towards the accurate deformation aspect (e.g., material characterization) (Delingette, 1998). The nature of this tradeoff is not well understood, and it is difficult to evaluate the relative performance of new systems when speed, accuracy, tissue properties and geometry all vary. For instance, modeling tissue surfaces proves to be faster, but less accurate than modeling tissue volumes (Cotin et al., 1996). Similarly, spring-mass systems have limited accuracy but work well in real-time (Waters, 1992; Kuhnapfel et al., 1997; Downes et al., 1998), while finite element (FE) modeling has proved successful for accurately modeling small deformations of linearly elastic materials where calculation speed is not a paramount concern (Bro-Nielsen and Cotin, 1996; Cotin et al., 1996).

FE modeling serves as a possible soft tissue validation tool for simple geometries and completely defined materi-

*Corresponding author. 29 Oxford St., Pierce Hall, Cambridge, MA 02138, USA. Tel.: +1-617-496-9098; fax: +1-617-495-9837.

E-mail addresses: kerdok@fas.harvard.edu (A.E. Kerdok), http://biorobotics.harvard.edu (A.E. Kerdok).

als and loading conditions. However, given that FE modeling is an approximation method in itself, the accuracy of its results heavily relies upon the quality of its input. Also, boundary conditions involving large deformations have difficulty converging when using FE modeling methods. Given these limitations, employing FE modeling to assess the accuracy of the various simplified algorithms used in real-time simulations of tissues with nonlinear material properties undergoing large deformations is of limited value.

It is the goal of this work to provide a method and preliminary data for quantifying the accuracy of soft tissue models. Towards this end we have developed a physical standard to assess the ability of an algorithm to precisely describe simulation of soft tissue under surgical manipulation. Ideally such a standard would take the form of stress, strain and displacement fields over the tissue surface and throughout the tissue volume for fully specified material properties, under a range of specified surgically relevant boundary conditions. The output of new modeling systems could then be compared to these standard physical results to validate and benchmark their performance (Fig. 1).

In this paper, we describe a practical physical standard for validation of soft tissue simulation. We used a 3D imaging technique to experimentally measure a well-characterized test phantom in the form of a cube of soft polymer. This 'truth cube' is made of a silicone rubber with fiducial spheres embedded in a 1 cm grid pattern throughout its $8 \times 8 \times 8$ cm^3 volume. We acquired computer tomography (CT) scans of the cube in undeformed and loaded states in both uniaxial compression and spherical indentation, and computed the relative displacement of each sphere using image processing techniques. These volumetric displacement results, along with details of the cube construction and boundary conditions in the two loading tests are reported. We also computed two FE

models to compare to the experimental results. Lastly, we conclude with a discussion of plans for extension of this work (including applying this method to biological tissues), and an invitation for participation by others interested in the validation of fast large-deformation tissue modeling.

2. Methods

We have selected a cube as a simple, regular shape to assess the feasibility of the validation approach and to develop the required techniques. The considerations include materials for the tissue phantom and fiducials, 3-D imaging, image processing and data reporting.

2.1. Truth cube

We chose a two-part silicone rubber (RTV6166, General Electric) for the cube because its behavior is similar to soft tissues in the linear range (Wellman, 1999; Ottensmeyer, 2001): the material is soft but exhibits linear behavior to at least 30% strain. To enable tracking of the internal deformation of the cube we embedded small spheres as fiducials that would readily appear in CT scans but not significantly alter the material properties of the silicone. The choice of sphere material and size was motivated by the need for high contrast without creating imaging artifacts (Strumas et al., 1998): this implies a specific gravity well above silicone (0.98) but much less than steel (~8). To enable accurate segmentation and position estimation, the minimum diameter of the spheres had to be slightly larger than the distance between two successive scanning planes (1.0–1.25 mm) but small enough to avoid compromising the material properties of the silicone. Imaging tests using several commercially available spheres of different materials and sizes embedded in a sample of the silicone gel revealed that Teflon spheres (specific gravity 2.3) with a diameter of 1.58 mm fulfilled all of these criteria.

The mold for the cube had removable sides, with the bottom serving as a rigid permanent mounting plate that was roughened and dimpled to ensure complete adhesion of the silicone. The two-part silicone rubber was mixed in a 30:70 proportion to obtain material characteristics similar to that of mammalian liver (Ottensmeyer, 2001). A layer 1 cm deep was poured, the mold was placed in a vacuum chamber to remove air bubbles, and then allowed to set on a level surface before positioning spheres in a 7×7 matrix spaced 1 cm apart (Fig. 2). The spheres were laid on the silicone rubber using a matrix of positioning tubes and allowed to set into the rubber before the next layer was poured. The end result produced a silicone rubber cube 8 cm on each side with 7 rows and 7 columns of Teflon spheres in 7 layers, spaced 1 cm apart in each direction (Fig. 2).
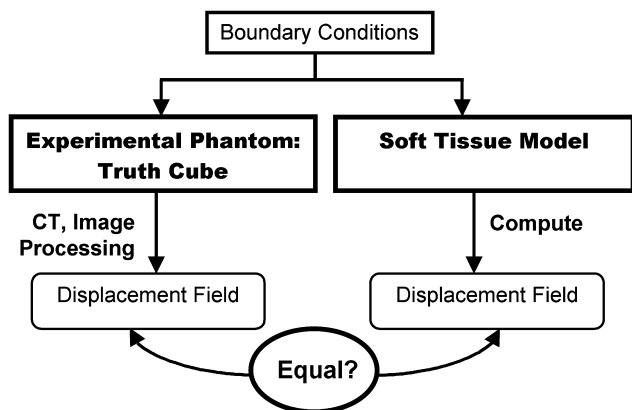

Fig. 1. Approach for validating soft tissue computational models. Boundary conditions (material property, geometric, loading conditions, etc.) are imposed on the experimental phantom and the model. The displacement fields in the phantom are measured using CT imaging and compared to the model's predicted results.
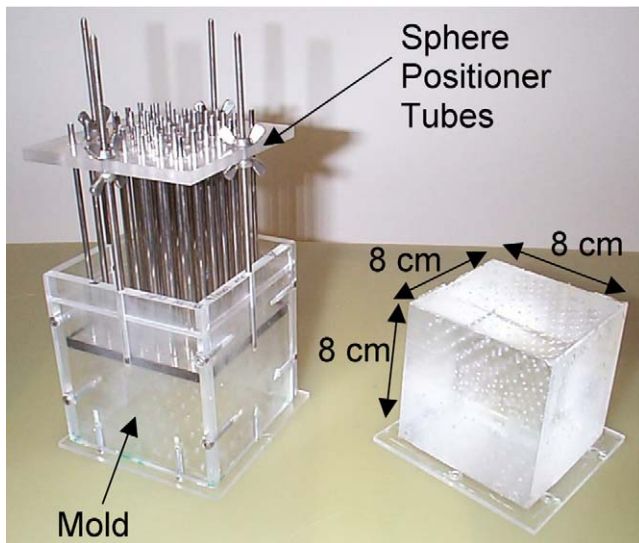
Fig. 2. Mold and internal sphere positioner (left) and resulting Truth Cube (right).

To ensure that the material properties of the silicone rubber were not affected by the addition of the 343 spheres, we performed indentation tests on three samples of the silicone rubber: alone, with sparse sphere density, and with 1 cm sphere spacing. Results indicated that the stiffness of the sample with the highest sphere density changed 2.0%, which is less than the 4.4% standard deviation of measurements of the plain sample. We thus conclude that the addition of the spheres had a negligible effect on the material properties of the silicone.

Both a small strain (<8%) uniaxial compression test and an indentation test were performed on a sample of the silicone rubber used to obtain material property charac-

teristics. Results indicate a Young's modulus of 15.0±0.4 kPa. Poisson's ratio is near 0.5 for this polymer consistent with many polymers.

2.2. Experimental set-up

The silicone rubber phantom with embedded fiducial markers (Teflon spheres) was initially imaged under uniaxial compression to allow us to develop the technique and compare the results to a fully defined FE model. A subsequent test used a spherical indentation loading condition more typical of surgical manipulations.

The experimental set-up loaded the cube under controlled boundary conditions during the CT imaging process (Fig. 3). The fixture base for the uniaxial compression test was constructed of 2.54 cm thick rigid plastic and had cutouts that exactly fit the base of the truth cube to ensure consistent alignment within the set-up. Registration markers (1.27 cm diameter Delrin spheres) were attached to the fixture base to allow for uniform positioning of the experimental set-up on the CT table between tests performed at different times under the same loading conditions (i.e., when the whole apparatus had to be moved). However, since we scanned each loading condition once without needing to change the experimental set-up between successive scans, these markers were mainly used as a visual assessment feature and as an estimate of overall scanner accuracy.

The initial loading test, uniaxial compression, was accomplished with a 2.54 cm thick acrylic plate. This compression plate was attached to a vertical support by a low-friction pivot. The plate was loaded by weights applied to the end opposite the pivot (in addition to the weight of the plate itself). The design confined all metal
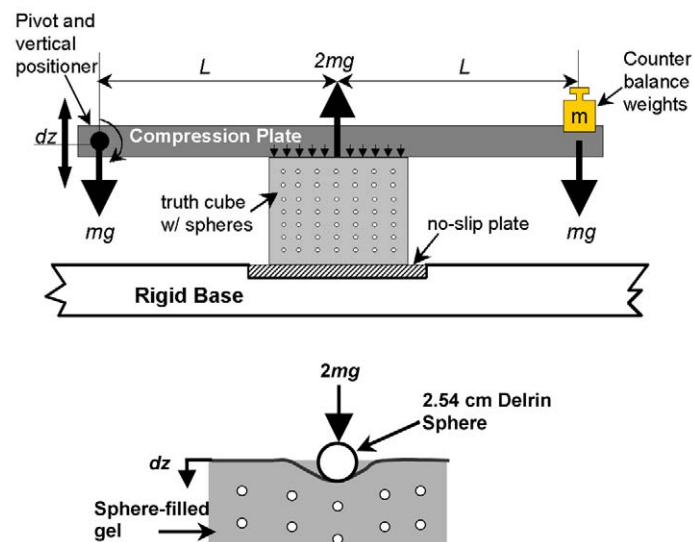

Fig. 3. Side view of the uniaxial compression experimental set-up (top) and close-up schematic of spherical indentation situation (bottom). L is the length from the loading points to the center of the cube, dz is the vertical motion, and m is the mass of the counter weights.

parts (the vertical support rods and weights) to the ends of the apparatus, so that they did not interfere with CT scanning of the cube in the middle of the apparatus. A linear dial indicator measured the distance the plate was translated (Fig. 4). A similar set-up was used for the large deformation spherical indentation test except that a 2.54 cm diameter Delrin spherical indentor mounted on a 1.9 cm diameter by 4.5 cm long Delrin cylinder was added to the compression plate (Fig. 4).

2.3. Experimental protocol

A first scan of the uniaxial compression experimental set-up was performed while the cube was unloaded to obtain a reference state of the internal sphere locations. The flat compression plate was then held level as it was lowered to a set displacement onto the oiled top surface of the cube. The oil was used to approximate a frictionless boundary condition. With the pivot end of the compression plate held in place, masses were added to a pocket in the other end until equilibrium was established as determined by level indicators. Three loading conditions were scanned: 4 mm, 10 mm, and 14.6 mm displacements, producing 5.0%, 12.5% and 18.25% nominal strain, respectively.

Once loaded, the cube was scanned in a General Electric LightSpeed CT scanner. Volumetric images of the truth cube were obtained using the following scanner settings: 120 kV, 180 mA, standard reconstruction type, and high quality scan mode. The field of view was 190 mm,

Fig. 4. Experimental test set-up for uniaxial compression (top) and spherical indentation (bottom).

producing a voxel size of $0.37 \times 0.37 \times 1.25$ mm^3. Each CT scan was composed of 99 slices, 1.25 mm thick (512×512 pixels, 16 bits), exported in DICOM format.

For the spherical indentation tests, the first scan was also conducted with the cube in an unloaded state for reference locations of the internal spheres. The compression plate with the indentor insert was then lowered in a manner similar to that of the uniaxial test. Two loading conditions were scanned: 18 mm and 24 mm displacements producing 22% and 30% local nominal strain, respectively. A third loading condition was attempted at 29 mm (36% nominal strain) but this caused the cube to fracture.

The indented cube was scanned in a similar manner and with the same settings as those used in the uniaxial compression test except that the field of view was 150 mm and a thinner slice thickness was used because a newer machine was made available that had better slice resolution (1.0 mm), producing a voxel size of $0.29 \times 0.29 \times 1.00$ mm^3. Each CT scan was composed of 133 slices, 1.0 mm thick (512×512 pixels, 16 bits) exported in DICOM format.

2.4. Image processing

Commercial software (3D-Doctor, Able Software, Lexington, MA) was used for manipulating the volumetric images. The minor artifacts present in the lower part of the cube (due to the support plate in the uniaxial compression test) were filtered. Then the internal spheres in each of the scans were segmented from the silicone rubber with thresholding; this was relatively straightforward due to the good contrast between the spheres and the silicone rubber. After segmentation of the 343 internal spheres a surface model of each sphere was calculated and exported as a 3D polygonal model.

The 1.58 mm diameter spheres embedded in the silicone cube have the size of several voxels (the voxel size is 0.37 mm or 0.29 mm for uniaxial compression and spherical indentation, respectively), so the 3D segmentation process only provided an approximation of the shape and location of the spheres. To accurately determine the location of the center of each internal sphere, we implemented a least-squares algorithm that fit an analytic sphere to the set of points defined by the vertices of the polygonal model of each sphere. This algorithm is integrated in visualization software we developed to display polygonal models and vector fields of the relative displacement of the embedded spheres' centroids from their unloaded states to the various loaded states. We manually matched the relative displacement vectors of the spheres' centroids between the various loading conditions. Finally, the surface of the cube at each compression stage was extracted from the images. The large external registration spheres were also segmented in order to evaluate potential motion of the entire experimental set-up between successive scans.
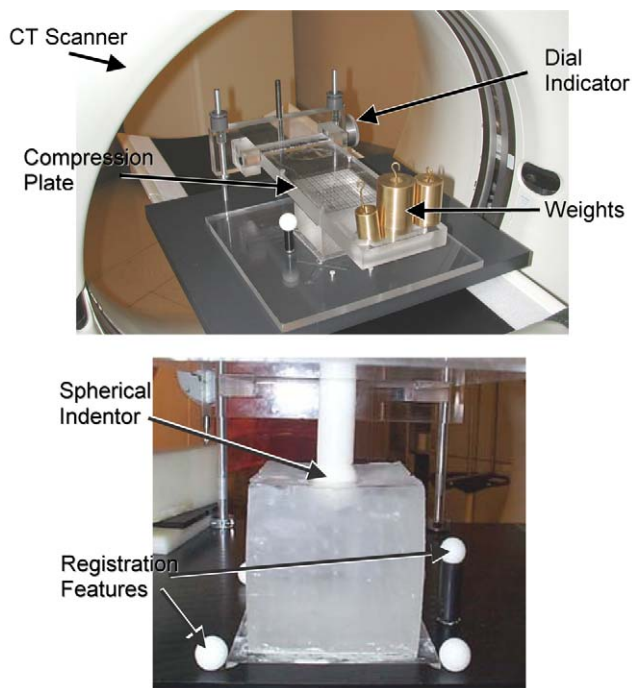
2.5. Finite element model

A finite element model of the truth cube using commercial FE modeling software (ABAQUS v. 5.8, Hibbitt, Karlsson & Sorensen, Pawtucket, RI) was developed to compare with the experimental results. A simple coarse mesh was created for the uniaxial compression test to emulate models used in real-time soft tissue simulations. A more refined model was created to compare to the large deformation spherical indentation test results.

For the uniaxial test, a mesh of $1\times1\times1$ cm^3, 8-node, solid hexahedral linear elements was created so that the nodes of this model corresponded to the Teflon spheres. For the spherical indentation test, the truth cube was meshed with 1134 solid axisymmetric triangular elements to represent the cube as a cylinder with an 8 cm diameter (Fig. 8). Representing the cube as a cylinder was a good approximation as a comparison of the sphere displacement versus radial position for an orthogonal cut and a diagonal cut through the cube image data showed negligible difference in the sphere displacement versus radial position. The models' material properties were isotropic and linear with a Young's modulus of 15 kPa and an assumed Poisson's ratio of 0.499. For the uniaxial case, large deformation (i.e., nonlinear) analysis was employed using the boundary conditions (frictionless upper surface, fixed lower surface, and free side surfaces) and geometry extracted from the CT scans for the unloaded and 18.25% nominal strain cases. For the spherical indentation case, large deformation (i.e., nonlinear), axisymmetric analysis was employed using the boundary conditions (fixed contact between indentor and upper surface, free side surfaces, and fixed lower surface) and geometry extracted from the CT scans for the unloaded and 22% nominal strain cases.

3. Results

Figs. 5 and 6 illustrate the processing of the uniaxial compression test and spherical indentation test data, respectively. Fig. 5 begins with segmented CT data for a vertical slice through the center of the cube, in both unloaded (Fig. 5A) and 18.25% strain (Fig. 5B) cases. Fig. 5C represents the relative displacement field for the central vertical slice across all strains. Reconstructions of the surface of the cube for each strain state are shown in Fig. 5D.

Fig. 6 begins with a CT of the center slice of the unloaded state (Fig. 6A) followed by the 30% nominal strain case (Fig. 6B) and the vector field of the center slice displacements (Fig. 6C). Reconstructions of the surface for the 30% strain state are shown in Fig. 6D.

As an estimate of scanner accuracy, physical measurements of the spherical registration features were compared to measurements made on the raw CT scans. These measurements suggest that the accuracy of the scanner is less than 0.1 mm. Minimal errors were introduced by our segmentation procedure on the internal spheres (thresholding, polygonal modeling, sphere fitting, centroid calculating and tracking). Comparing the internal sphere location from raw to segmented data suggest that the error of the sphere locations is less than the size of one voxel in plane and less than half the size of the slice thickness out of plane. Therefore the estimated overall error in plane for the uniaxial compression and spherical indentation data are less than 0.37 mm and 0.29 mm, respectively, and less than 1.25 mm and 1.0 mm out of plane.

The predicted results from the center slice of the FE model of the simple uniaxial compression test are shown in Fig. 8A. There is a 3.5 mm maximum difference from the experimental results for a top surface displacement of 14.6 mm (18.25% nominal strain). The results predicted from a center slice of the more refined spherical indentation FE model at 22% nominal strain (18 mm displacement) are shown in Fig. 8B. Fig. 7 compares the internal sphere displacement results of the FE model to the measured data at 22% nominal strain for the spherical indentation case. The maximum difference between the model and the test results is 1.7 mm. This FE model was unable to converge at 30% nominal strain.

4. Discussion

This study demonstrates a technique for creating physical standards for validating the accuracy of real-time soft tissue simulation models. It was our goal to show that experimentally measured local internal displacement data from soft materials serves as a means of validating these models.

Our ideal physical standard would provide measurements of the deformation and stress fields over the surface and throughout the volume of soft tissues under large deformations ($>$30% strain) typical of surgical manipulation. This physical standard would also need to have well-characterized material properties similar to the simulated tissue, surgically relevant specified boundary conditions, and known geometry. Our truth cube has a modulus in the range of liver, $E\sim15$ kPa as reported by Ottensmeyer (2001). Imaging at strains of over 30% was easily accomplished. The external surface and the embedded fiducial spheres were readily segmented, which permitted calculation of the relative displacement fields throughout the volume. The result is a local displacement data set with well-characterized material properties and boundary conditions that can be used to assess the precision of soft tissue models under similar situations. Full displacement results and raw CT scans of both experiments are available on the project web site.

FE modeling is currently used to check the accuracy of soft tissue simulation models. We also compared our results to the output of these computational models. The
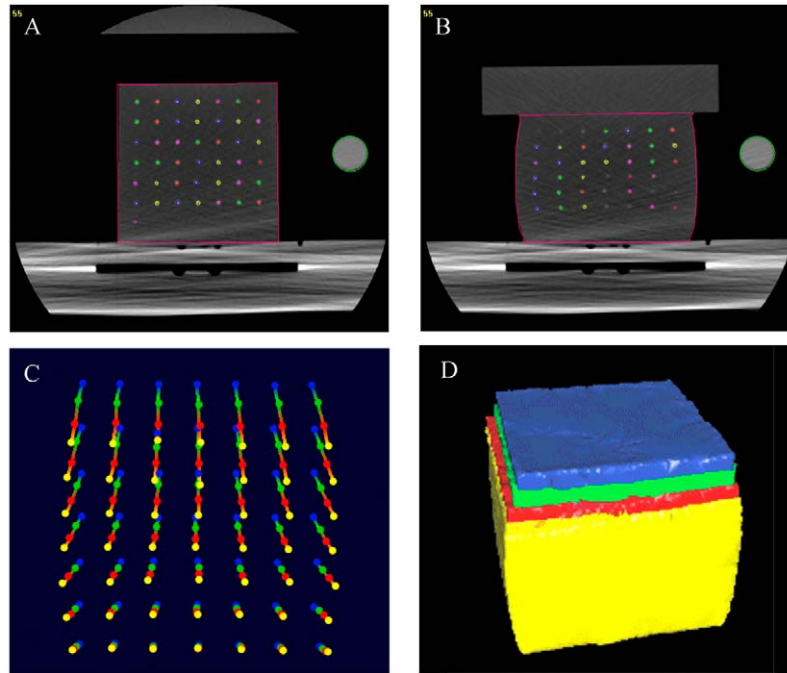
Fig. 5. The CT image of the central vertical plane of the Truth Cube after segmentation in both the unloaded (A) and maximally uniaxial compressed (B) states. Note the registration marker off to the side. Internal sphere trajectory and location in the central plane (C) (blue = unloaded, green = 5%, red = 12.5%, yellow = 18.25% strain). Outer surface of the cube in its four strain states (D).

simple FE model calculation presented for the uniaxial compression test used a minimal number of elements to reflect some of the speed versus accuracy tradeoffs of

real-time tissue simulations. While the FE modeling and experimental data showed qualitative agreement, even with these simple loading conditions on a linearly elastic
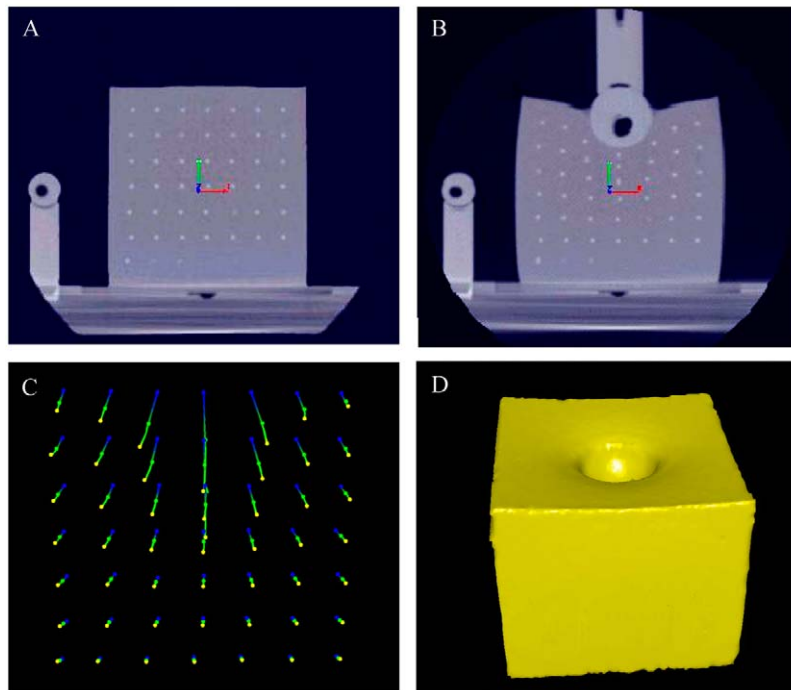

Fig. 6. CT of center vertical slice for spherical indentation in unloaded state (A) and under 30% nominal strain (B). Note the registration marker off to the side. The trajectory and locations of the internal spheres for the same slice is shown in (C) where blue represents no indentation, the 22% nominal strain case is shown in green, and the 30% nominal strain case in yellow. The surface for the 30% strain case is represented in (D).
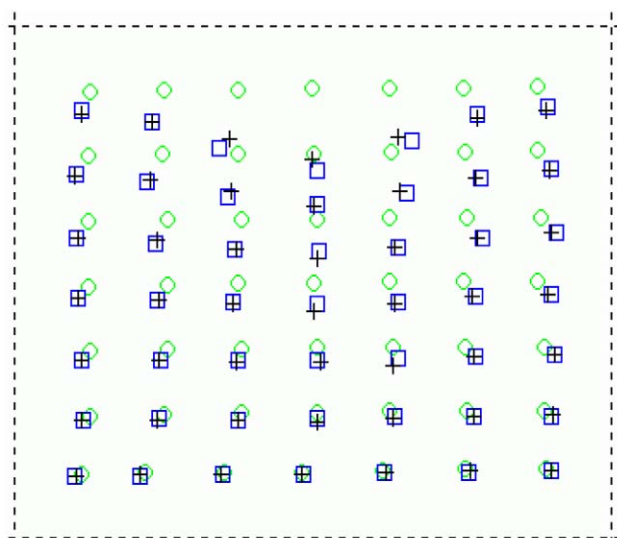
Fig. 7. Comparison of the measured internal sphere displacement (boxes) versus the FE model's predicted sphere displacement (crosses) for the 22% nominal strain spherical indentation case. The circles are the original internal sphere locations and the dashed line is the undeformed outer surface.

material the maximum single-point differences between the model and the experimental results were 3.5 mm for the 14.6 mm uniaxial displacement. Such an error may have significant consequences for applications such as surgical planning. Some portion of the difference may be due to inexact specification of the boundary conditions on the top of the cube during compression as well as the experimental error. Refinement of the model (e.g., smaller mesh size) should bring closer agreement to the experiment at the expense of increased computation time.

For the spherical indentation situation a finer resolution mesh was used to better replicate the experimental results. The maximum single-point differences between the model and the experimental results were relatively small (1.7 mm) for the 18 mm indentation case The model failed to converge for the 26.4 mm indentation situation (30% nominal strain) that was experimentally measured, and so no comparison could be drawn for this larger deformation. This demonstrates one of the limitations of using FE modeling as a validation tool: even the most robust FE models do to not readily converge for large deformations of the complex materials typically seen in surgical manipulations (Szekely et al., 2000).

Strains larger than 30% may be expected in surgical situations on biological tissues, i.e., organ retraction. Current FE modeling techniques for dealing with such gross deformation such as regridding are difficult to implement and of uncertain accuracy. This emphasizes the need for physical models as validation standards. We therefore conclude that although FE modeling is a powerful tool it may not be the most appropriate means of validating real-time soft tissue simulation models. The truth cube technique, however, results in an experimentally measured internal strain field with good resolution for all material properties, and thus should be the validation method of choice.

Several refinements to the measurement techniques are indicated by these results. First, we have only estimated the accuracy of the local internal sphere positions in this initial dataset. More precise accuracy specifications can be obtained through an analysis of the imaging and image processing procedures, and through reproducibility measurements. The raw scan data is available on the web site, so readers are welcome to develop improved image processing algorithms for this purpose. Another area for better characterization is the top surface boundary condition, where oiling the cube served to limit and regularize friction, but where a truly 'frictionless' condition did not apply. Fortunately, the contact area is readily measured during the experiment and in the processed CT images, so additional boundary information is available.

5. Future work

This initial study demonstrated the feasibility of experimental measurement of volumetric displacement fields for soft material phantoms under large strains, and provides some useful internal strain field data that can readily be used to validate soft tissue models. The truth cube has regular geometry and well-characterized material properties and loading conditions that was helpful for the development process, but fast tissue simulations must deal with conditions that are vastly different, involving very large deformations, irregular shapes and complex materials.

The next phase of this project is thus the measurement of biological tissue volumetric displacements, in the form of an entire organ. Preliminary plans call for measurement of a porcine liver immediately post mortem. We will determine the best ways to impose internal markers in the organ while minimizing damage to the tissue or affecting the material properties of the tissue, and to develop appropriate testing situations where the boundary conditions are completely identified. As an initial trial, 7 rows and 6 columns of the Teflon spherical fiducials were inserted in two layers about 2 cm deep via saline-filled blunt needles throughout a portion of the parenchyma of a freshly excised bovine liver. This liver was then imaged using the standard abdominal/pelvic settings for a human liver in an unloaded and a fully retracted state (strains >30%). This state is similar to how a surgeon would bend the liver out of the way to gain access to abdominal structures below. The results shown in Fig. 9 (the experimental set-up followed by CT slices of the unloaded and retracted liver) suggest that only minor modifications
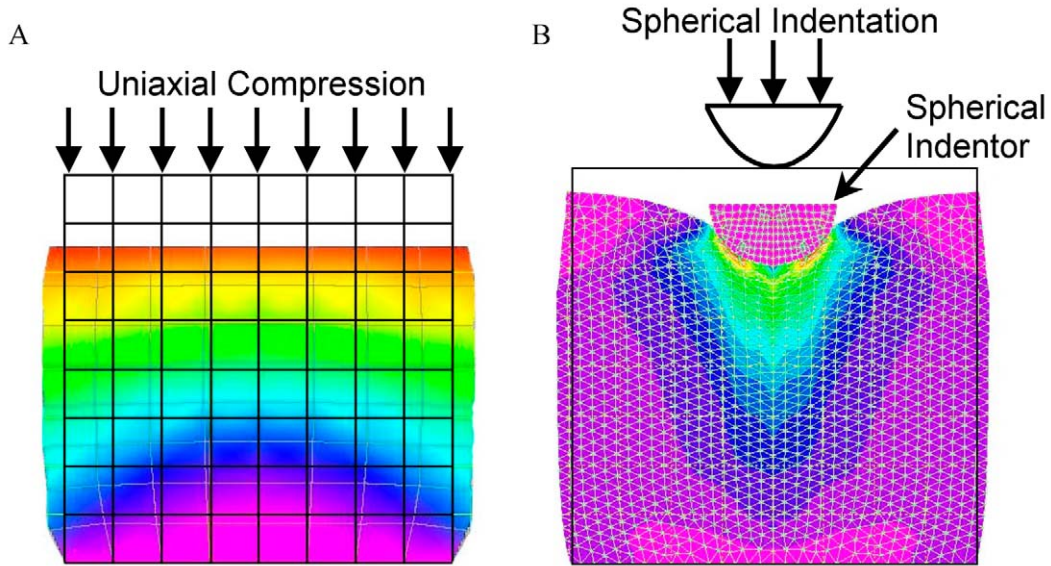
Fig. 8. Center slice of the uniaxial compression coarse mesh under 18.25% strain (A). Center slice of the refined spherical indentation FEM mesh displaying the results of the 22% strain experiment (B). The magnitude of the strain is coded as color with red indicating the highest strain and violet indicating the lowest. Note that the undeformed model is outlined in black.

to our current technique will be needed to obtain volumetric data of real soft tissue.

While these biological material tests have obvious advantages, the material properties will not be well-char- acterized as in the phantom tests. The identification of these material properties is an active area of research, and the data sets may be useful for solving the inverse problem of estimating these material properties from the displace-
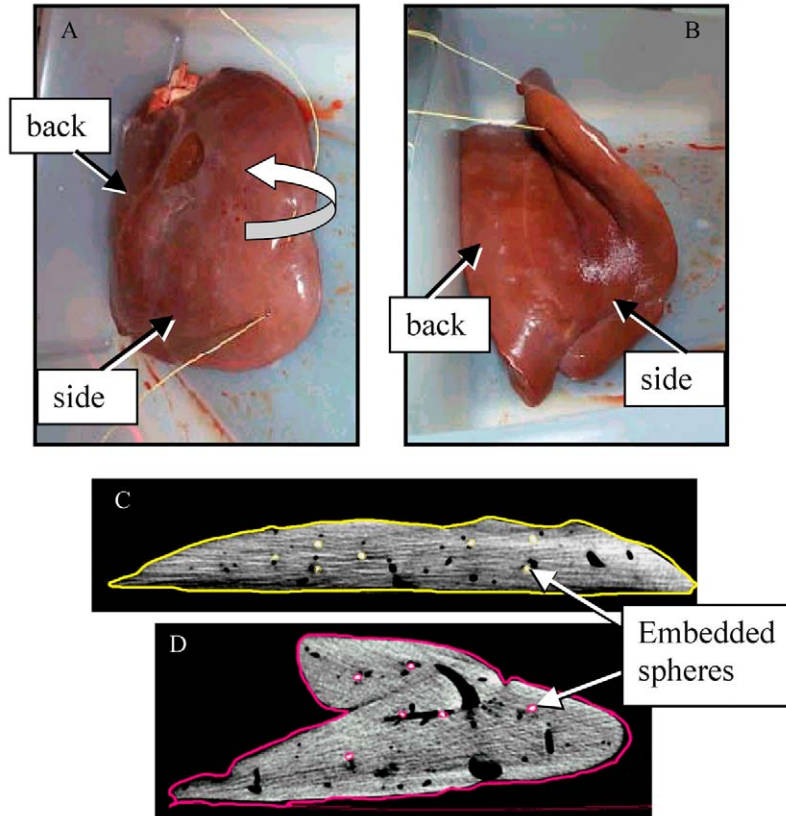

Fig. 9. Bovine liver retraction experimental set-up and results. The liver was cut to size, embedded with Teflon spheres, and imaged in the unloaded (A) and retracted (B) states. CT slices of the undeformed (C) and of the retracted liver (D). Spheres and surfaces are highlighted.

ment data. In any case, the displacement data alone will provide a source of information for the development and validation of fast simulation systems.

As we proceed, we welcome comments and suggestions on all aspects of the project, from tissue selection and loading conditions to experimental methods and data analysis. Further information is provided on the web site at: http://biorobotics.harvard.edu/truthcube (soon to be www.truthcube.org). Contributions of a broad cross-section in the tissue modeling community will help ensure the development of a robust physical standard for the benchmarking of real-time soft tissue simulations.

Acknowledgements

References

Bro-Nielsen, M., Cotin, S., 1996. Real-time volumetric deformable models for surgery simulation using finite elements and condensation, Eurographics '96-Computer Graphics Forum 15, 57–66.

Cotin, S., Delingette, H., Clement, J.M., Bro-Nielsen, M., Ayache, N., Marescaux, J., 1996. Geometrical and physical representations for a simulator of hepatic surgery. In: MMVR '96. IOS Press, Amsterdam, The Netherlands, pp. 139–150.

Delingette, H., 1998. Towards realistic soft tissue modeling in medical simulation. IEEE: Special Issue in on Virtual and Augmented Reality in Medicine 86, 1–12.

Downes, M., Cavusoglu, M., Gantert, W., Way, L., Tendick, F., 1998. Virtual environments for training critical skills in laproscopic surgery. In: MMVR '98. IOS Press, Amsterdam, The Netherlands, pp. 316–322.

Kuhnapfel, U.G., Kuhn, C., Hubner, M., Krumm, H.G., MaaE, H., Neisius, B., 1997. The karlsruhe endoscopic surgery trainer as an example for virtual reality in medical education. Minim. Invasive Ther. Allied Technol. 6, 122–125.

Ottensmeyer, M.P., 2001. Minimally invasive instrument for in vivo measurement of solid organ mechanical impedance. PhD Thesis, Department of Mechanical Engineering, Massachusetts Institute of Technology Cambridge, MA.

Strumas, N., Antonyshyn, O., Yaffe, M.J., Mawdsley, G., Cooper, P., 1998. Computed tomography artifacts: an experimental investigation of causative factors. Can. J. Plast. Surg. 6 (1), 23–29.

Szekely, G., Brechbuhler, C., Dual, J. et al., 2000. Virtual reality-based simulation of endoscopic surgery. Presence 9 (3), 310–333.

Waters, K., 1992. A physical model of facial tissue and muscle articulation derived from computer tomography data. Visualization in Biomedical Computing. Chapel Hill, NC. In: SPIE Proc. VBC'92.

Wellman, P.S., 1999. Tactile imaging. PhD Thesis, Division of Engineering and Applied Sciences, Harvard University Cambridge.